Artificial Protection Film on Lithium Metal Anode toward Long-Cycle-Life Lithium–Oxygen Batteries

Qing-Chao Liu, Ji-Jing Xu, Shuang Yuan, Zhi-Wen Chang, Dan Xu, Yan-Bin Yin, Lin Li, Hai-Xia Zhong, Yin-Shan Jiang, Jun-Min Yan, and Xin-Bo Zhang*

Development of lithium metal anode with superior stability plays a vital role in improving the cycle life of rechargeable lithium–oxygen (Li–O_2) battery. Herein, we design and fabricate a stable solid electrolyte interphase film on the lithium metal using a facile electrochemical generation strategy. X-ray photoelectron spectroscopy demonstrates that the obtained artificial film on Li metal surface contains lithium carbonate, lithium fluoride and polyene, as well as C–F bond-containing compounds. Unexpectedly, in a proof-of-concept experiment, even using conventional commercial carbon (super P) as cathode, the as-obtained protected lithium anode endows the Li–O_2 battery with superior cycle stability—more than 100 stable cycles is obtained under a fixed capacity of 1000 mA h g^{-1} at a current density of 300 mA g^{-1}, which is more than three times that of the Li–O_2 battery with the pristine Li metal as an anode (31 cycles). This significant enhancement of the cycling stability could be attributed to the artificial protective film, which effectively protects the Li metal from corroding of organic solvent and dissolved O_2 during discharge–charge cycles.

With increasing environmental concerns and accelerated depletion of fossil fuel, development of electric vehicles (EVs) cars has received intensive attentions. Although lithium-ion batteries (LIBs) have been widely used in portable electronic devices, we shall always think of limited energy density of LIBs, which significantly hinders the increase of driving range of EVs on a single charge.[1–9] In response, rechargeable Li–O_2 batteries have recently attracted a great deal of attention because of their extremely high specific energy density according to the electrochemical reaction (2Li + O_2 + 2e$^-$ ⇌ Li$_2$$O_2$, 2.96 V vs Li/Li$^+$), which is nearly ten times that of conventional LIBs.[10–17] However, to enable Li–O_2 batteries for practical applications, numerous scientific and technique challenges are urgently needed to be overcome,[18] including instability of electrolyte,[19] air cathode and especially the lithium metal anode.[20,21] Recent reports have clearly demonstrated that the Li metal as anode in Li–O_2 batteries could readily react with the electrolyte especially in the oxygen-containing environment,[21a] and this would inevitably consume electrolyte and finally lead to short cycle life due to premature death of Li–O_2 batteries.[1,22,23] Adding insult to injury, the undesirable growth of dendritical lithium on the Li metal anode surface upon cycling would inevitably cause serious safety problems. In response, very recently, a few approaches for improving the stability of the pristine Li anode in Li–O_2 batteries have been reported,[24–28] including using special electrolyte and additive, coating a protective polymer layer, soaking with organic solvent, and even replacing Li anode with low potential and high capacity silicon alloy anode material. Although these strategies alleviate the Li corrosion to some extent, they are still far from satisfying in terms of requirement of high cost and the complex treatment process, instability of the formed protection film, and especially when further considering the fact that enhancement in cycle life of Li–O_2 batteries is still very limited. Therefore, development of a novel strategy to effectively protect the Li metal anode to significantly improve the cycle stability of Li–O_2 batteries is highly desirable yet still very challenging.

Herein, we first propose and realize a facile while very effective strategy to protect the Li anode through artificially fabricating a protection film on the metal Li, wherein the fluoroethylene carbonate (FEC) plays a key role as a crucial film-forming additive. Surprisingly, as a proof-of-concept experiment, when even employing conventional Super P as cathode, the obtained FEC-treated Li metal (F-TLM) anode endows Li–O_2 batteries with superior cycle stability—more than 100 stable cycles with a fixed capacity of 1000 mA h g^{-1} at a current density of 300 mA g^{-1} is obtained, which is more than three times that of the cells with the pristine Li metal (PLM) and Li metal (TLM) treated without FEC as anode. The significantly improved cycling stability could be attributed to the artificial protective film derived from FEC decomposition, which is found to be composed of Li$_2$CO$_3$, LiF, polyene, and C–F bond-containing compound and thus effectively protects the Li metal anode from corroding of organic solvent and dissolved O_2, highlighting the feasibility and strength of our strategy.

Scheme 1 shows the fabrication process of the artificial protective film on Li metal by using an electrochemical strategy. In brief, the protective film is formed by charging a symmetric Li/electrolyte/Li cell within a voltage window of 0–0.7 V at a scan rate of 1 mV s^{-1} for several cycles, wherein the electrolyte is 1 M LiF$_3$SO$_3$ dissolved in tetraethylene glycol dimethyl

Q.-C. Liu, S. Yuan, Y.-B. Yin, L. Li,
Prof. Y.-S. Jiang, J.-M. Yan
School of Materials Science and Engineering
Jilin University
Changchun 130012, China
Dr. J.-J. Xu, Z.-W. Chang, Dr. D. Xu, H.-X. Zhong,
Prof. X.-B. Zhang
State Key Laboratory of Rare Earth Resource Utilization
Changchun Institute of Applied Chemistry
Chinese Academy of Sciences
Changchun 130022, P. R. China
E-mail: xbzhang@ciac.ac.cn
Z.-W. Chang
University of Chinese Academy of Sciences
Beijing 100049, China
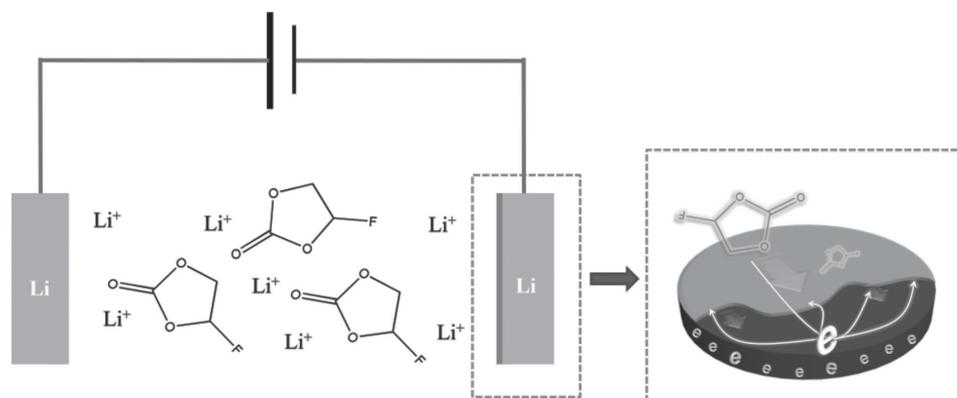
Scheme 1. Schematic illustration of the formation of protective film on Li anode using an ex situ electrochemical strategy.

ether (TEGDME)-FEC (5:1 v/v). Then, the symmetric cell is disassembled and the Li anode is employed for Li–O$_2$ batteries. For comparison, the electrolyte without FEC is also used in this work. Photographic images of PLM (left), TLM (middle), and F-TLM (left) are shown in Figure S1 (Supporting Information). Compared to the PLM and TLM, the surface of the F-TLM is obviously covered with a layer of dark film, implying the successful formation of the protective film on the Li metal anode.

In order to investigate the composition of the dark film, the X-ray photoelectron spectroscopy (XPS) technique is employed. **Figure 1**a–d shows the XPS spectra of Li 1s, O 1s, C 1s, and F 1s

for the metal Li after electrochemical treatment with 1 M LiF$_3$SO$_3$ in TEGDME-FEC electrolyte. As shown in Figure 1a, the XPS spectra of Li 1s can be deconvoluted into two Gaussian component peaks at 55.3 and 56.0 eV, which can be assigned to lithium carbonates and lithium fluoride (LiF), respectively. Figure 1b displays the O 1s spectrum, which can be fitted into two peaks centered at 531.0 and 532.0 eV—the latter peak could be assigned to carbonate species while the former might be ascribed to adsorbed oxygen species. Combining with Li 1s and O 1s spectra, the existence of lithium carbonate (Li$_2$CO$_3$) in the generated artificial protection film could be concluded. As

Figure 1. The Li 1s, O 1s, C 1s, and F 1s XPS spectra of F-TLM anode.
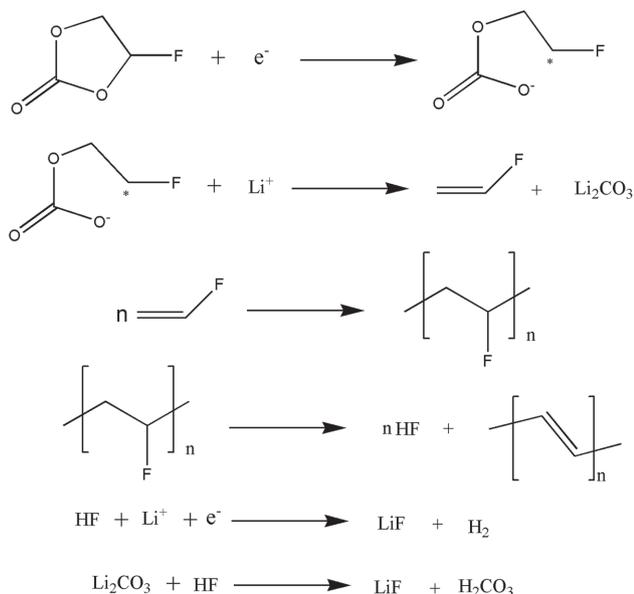
Figure 2. The proposed formation mechanism of the protective film on Li anode.

respectively. Furthermore, as for F 1s spectrum (Figure 1d), the two peaks located at 689.2 and 685.5 eV could be assigned to C–F bond-containing compound (derived from the polymerized C–F molecule) and LiF (also considering the Li 1s peak at 56.0 eV), respectively. In sharp contrast, when FEC is not added in the electrolyte (1 M LiF$_3$SO$_3$ dissolved in TEGDME), formation of LiF could not be found from the XPS spectrum (Figure S2, Supporting Information), showing that FEC plays critical role in the formation of LiF-containing film on Li metal.

Based on these obtained XPS results, we then propose a preliminary mechanism for the formation of the artificial protection film on Li metal anode as displayed in **Figure 2**. First, the electrolyte additive, FEC molecule, is decomposed into C–F molecule and Li$_2$CO$_3$ via obtaining Li$^+$ and e$^-$, and then the generated C–F molecules are polymerized, forming C–F polymer. Some C–F polymer become a component of the protective film, while the others are decomposed to polyene compound and HF, of which the former also constitutes the protective film, while the latter could partly react with the obtained Li$^+$ and e$^-$ at the active reductive Li metal surface to form LiF and H$_2$. In addition, the remaining HF could also react with some part of the Li$_2$CO$_3$, forming LiF and H$_2$CO$_3$. Therefore, the artificially generated protection film consists of Li$_2$CO$_3$, LiF, polyene, and C–F bond-containing compound.[29]

Inspired by the successful formation of the LiF-containing protective film on Li anode, we then investigate its effect on the electrochemical stability of protected Li anode surface. To this end, linear sweep voltammetry (LSV) technology is applied to investigate the reaction between Li anode and electrolyte.[24] The

shown in Figure 1c, the C 1s spectrum could be deconvoluted into three peaks centered at 284.6, 284.8, and 289.4 eV which are corresponding to C–C, C–H, and C=O functional group, respectively. Based on above results, the C–H and C=O functional groups might be related to polyene and carbonate groups,
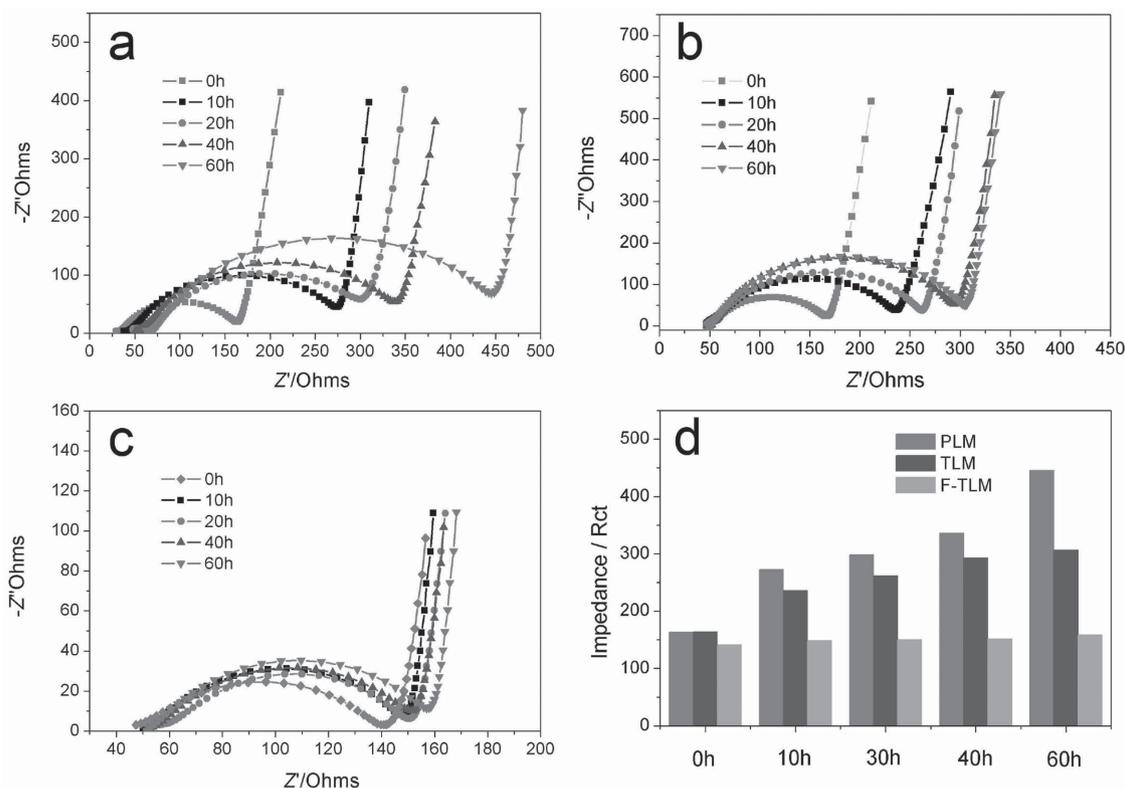
Figure 3. Time dependence of the impedance spectra of the Li–O$_2$ cells with a) PLM, b) TLM, or c) F-TLM as anode, and d) their corresponding impedance values.

LSVs of the three pristine (without predischarge process) Li–O$_2$ cells using the PLM, TLM, and F-TLM as anodes are shown in Figure S3 (Supporting Information). It can be found that strong oxidation peaks positioned about 4.0 V are observed for the Li–O$_2$ cell with PLM or TLM anode, which can be attributed to the reaction between Li anode and electrolyte.[21a] In sharp contrast, the Li–O$_2$ cell with F-TLM anode substantially inhibits the production of these electroactive species and finally effectively protects the Li anode. In order to further investigate the effect of the LiF-containing protective film on Li anode surface in real Li–O$_2$ cells, the time-dependence electrochemical impedance spectra of the Li–O$_2$ cells with PLM, TLM, and F-TLM as anodes are displayed in **Figure 3**a–c, respectively. Figure 3d demonstrates their corresponding impedance value. It could be found that with time prolonging, the impedance of Li–O$_2$ cell with PLM or TLM as anode increases sharply, while almost

no significant impedance change is observed even after 60 h in the Li–O$_2$ cell with F-TLM anode, which should be attributed to the protection effect of the artificial generated protection LiF-containing film on Li anode in terms of preventing the Li anode from corroding by electrolyte or/and dissolved O$_2$ as it could inevitably increase the resistance of the Li–O$_2$ cell. All these results further confirm the efficacy of the protective film in effective improving the stability of Li anode in Li–O$_2$ cell.

To study whether the F-TLM anode could improve the stability of Li–O$_2$ cells upon continuous discharging/charging processes, the cycling performances of Li–O$_2$ cells with the three kinds of anodes (PLM, TLM, and F-TLM) are presented in **Figure 4**. Figure 4a,c,e shows the discharge–charge curves of the Li–O$_2$ cells with different Li anodes, respectively. Figure 4b,d,f is the corresponding terminal-potential profiles of these Li–O$_2$ cells. It could be clearly found that the Li–O$_2$ cells
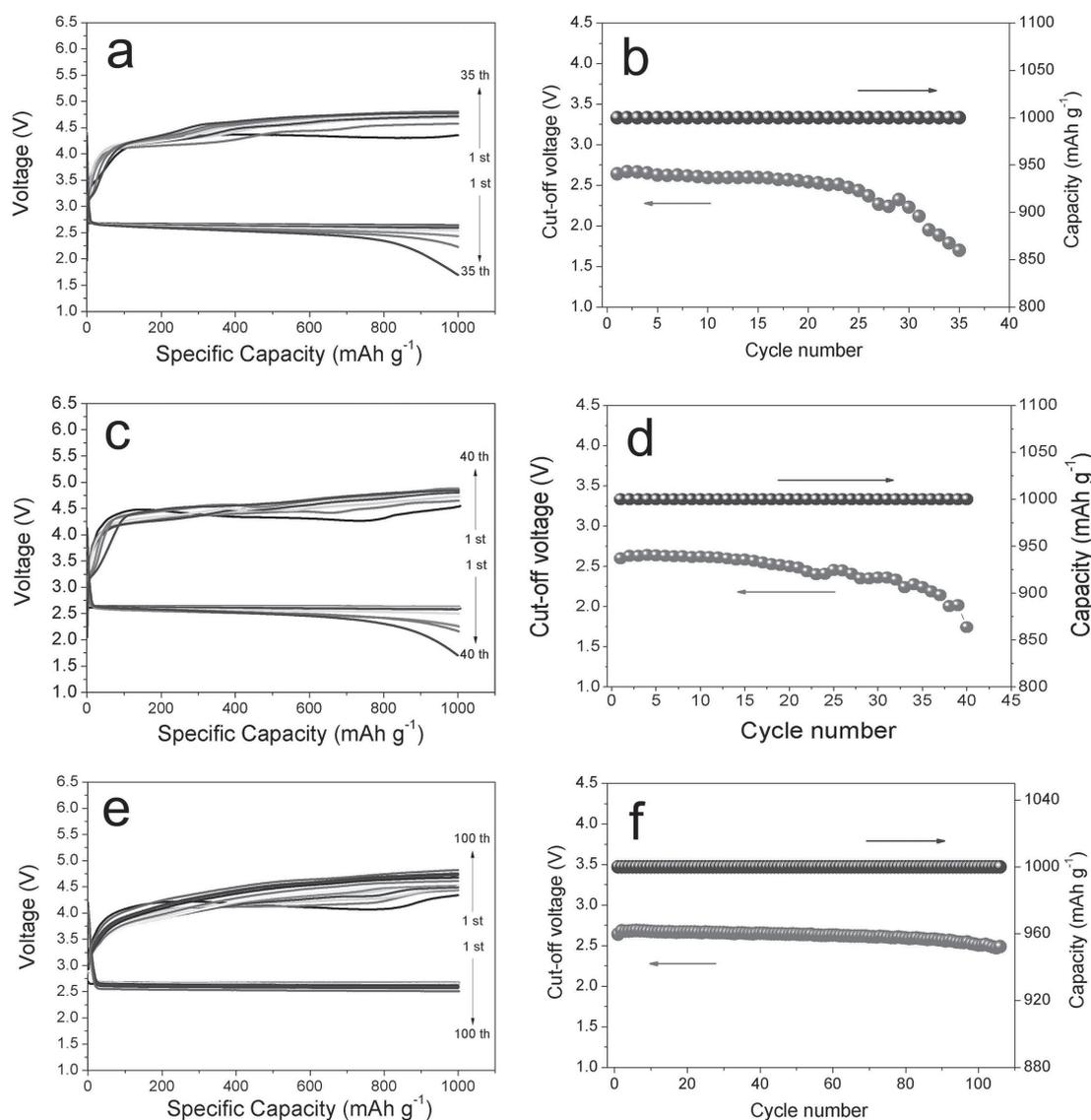
Figure 4. Discharge–charge curves of Li–O$_2$ cells with a) PLM, c) TLM, or e) F-TLM anode, and the corresponding cycling performance b,d,f) with a fixed capacity of 1000 mA h g^{-1} at a current density of 300 mA g^{-1}.

with PLM or TLM as anode could only cycle for 31 and 39 cycles with the cut-off voltage restricted to 2.0 V, respectively. Unexpectedly, the Li–O$_2$ cell with protected F-TLM anode can cycle more than 100 cycles (Figure 4f). This significantly enhanced cycling performance is believed to be derived from the effective suppression of Li metal anode corrosion by the LiF-containing protective film. To further evaluate this enhancement effect, the capacity of the Li–O$_2$ cells with PLM, TLM, or F-TLM anode is increased to 2000 mA h g^{-1} even at a current density of

300 mA g^{-1} (Figure S4, Supporting Information). Similarly, the cells with PLM or TLM anode show a rapid decay of the cut-off voltage. At the terminal voltage of 2.0 V, the cells could run no more than 18 and 24 cycles, respectively. In sharp contrast, the cell with F-TLM anode can still stably run for 38 cycles, highlighting once more the effectiveness of our protection strategy.

It should be noted that besides the lithium anode, electrolyte and cathode could also play an important role in cycling stability of Li–O$_2$ cells. In order to separate the influence of Li
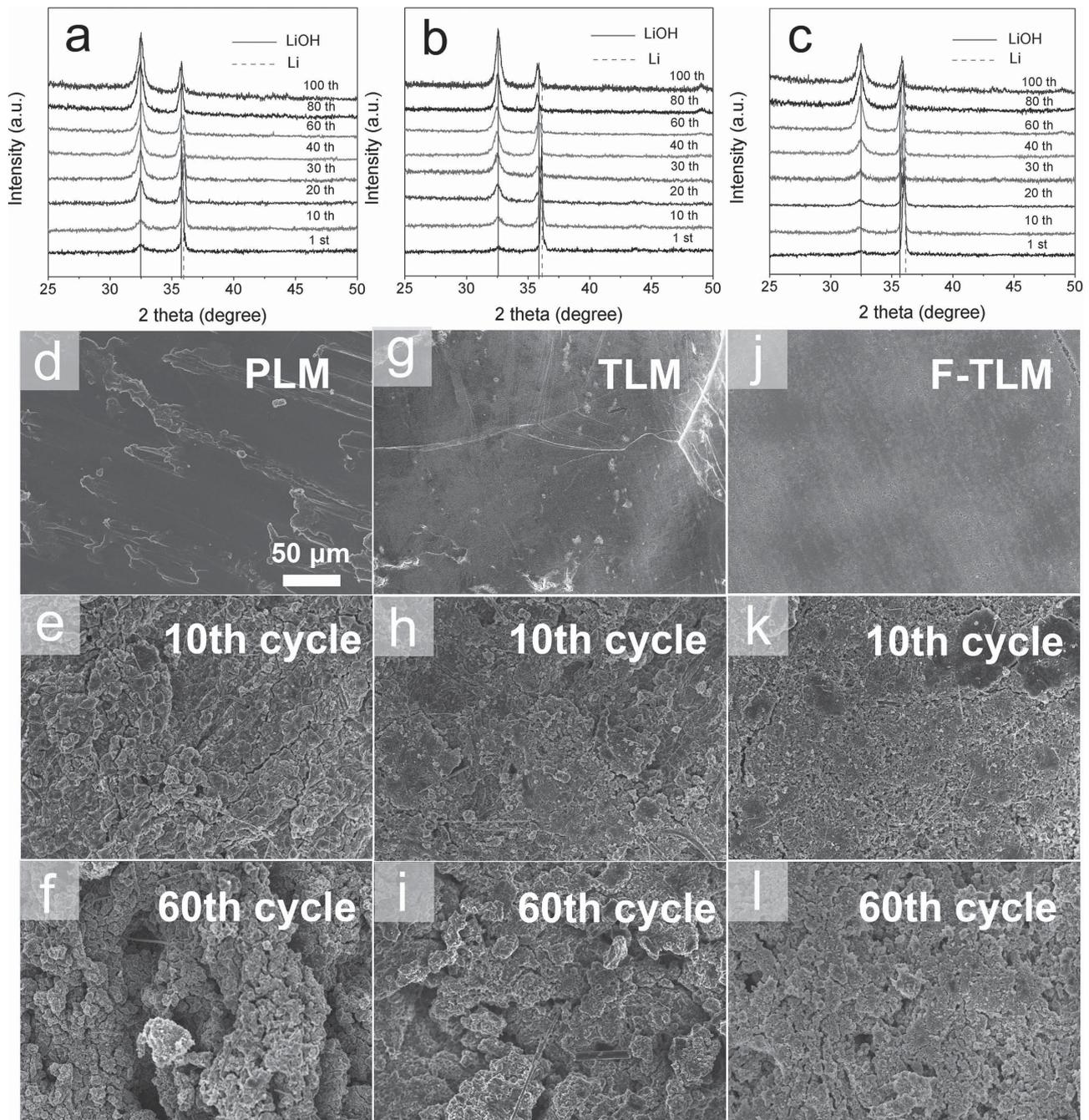
Figure 5. Representative ex situ XRD patterns taken from the a) PLM, b) TLM, and c) F-TLM anodes at different cycles. SEM images of PLM anode morphologies evolution d) before cycle, e) tenth cycle, and f) 60th cycle. SEM images of TLM anode morphologies evolution g) before cycle, h) tenth cycle, and i) 60th cycle. SEM images of F-TLM anode morphologies evolution j) before cycle, k) tenth cycle, and l) 60th cycle.

anode on cycling performance from factors derived from other cell components, we "rebuilt" Li–O$_2$ cells with new cathode/separator and fresh electrolyte but using the used Li anodes taken from the previous failure cells. With the aim of more effectively exhibiting the protection effect on the Li anode, we restricted the capacity to 2000 mA h g^{-1} under the current density of 300 mA g^{-1} in the following experiments. Interestingly, as shown in Figure S5 (Supporting Information), by changing the cathode, separator, and electrolyte, the cycling life of all the three cells could be significantly enhanced (Figure S4, Supporting Information), further confirming that cathode, separator, and electrolyte could affect the cycling life of Li–O$_2$ cells. However, it should be noted that the cycle life of the cell with F-TLM anode is still much better than the two counterparts, indicating that the artificial film could protect the Li metal from fast corrosion, which further demonstrates that the strategy of Li anode protection can effectively improve the cycling stability of Li–O$_2$ cell. Surprisingly, it is found that, if we further continue the discharge–charge tests, an unreported new stable state gradually emerges for all the failed three cells, while the discharge and charge curves are not the characteristic profiles of a Li–O$_2$ battery.

To further understand the underlying mechanism of the above-obtained improved electrochemical performances, we then investigate the composition changes on the pristine and protected Li anode surface. The amount of LiOH formed on the Li metal surface is generally employed as a standard index of the degree of corrosion of anode.[21b] After the first discharge–charge cycle, XRD diffraction peaks of LiOH on PLM and TLM anodes can be found clearly (**Figure 5**a,b). In sharp contrast, the peaks of LiOH are much weak for F-TLM anode (Figure 5c). Although the peaks of LiOH gradually emerge on the F-TLM anode in the following cycles, the intensity of LiOH peaks is always much weaker than these on PLM or TLM anode, which might indicate that the amount of LiOH formed on the F-TLM anode is less than that formed on the PLM or TLM anode. Furthermore, the growth rate of LiOH on the PLM or TLM anode is much faster than that on the F-TLM anode, showing the protective film on the F-TLM anode can effectively suppress the parasitic reactions on the Li anode/electrolyte interface, thus improving the Li–O$_2$ electrochemical performance (vide supra). The morphology evolution of the three different anodes is then investigated (ten and 60 cycles). Before discharge–charge cycle, compared to that of the PLM (Figure 5d) and TLM (Figure 5g), the surface of F-TLM anode is much smoother (Figure 5j) due to the artificially formed compact layer (Li$_2$CO$_3$, LiF, polyene compound, and C–F bond-containing compound) on the Li metal surface. Furthermore, compared to that of F-TLM anode, the surface of PLM and TLM anode becomes much rougher and large holes can be observed with the prolonged cycling, indicating that the protective film formed on the Li anode significantly suppresses parasitic reactions at the Li anode/electrolyte interface. It should be noted that the formed protective film on Li anode does not influence the main discharge product (Figure S6, Supporting Information)—the primary discharge product is Li$_2$O$_2$ and the morphology is typical toroidal, which has been reported by many other groups.[30–38]

In summary, a novel artificial LiF-containing protection film is first obtained on very reactive Li metal by a facile while very effective electrochemical strategy, wherein the FEC is employed as a crucial electrolyte additive for the stable film formation. Unexpectedly, as a proof-of-concept application, when the protected metal lithium is used as novel anode for Li–O$_2$ battery, significantly improved cycling stability (up to 106 cycles) is obtained even using conventional unoptimized Super P as cathode, which is more than three times that of the Li–O$_2$ battery with the pristine Li metal as an anode (31 cycles). Coupled with the results of XRD and the surface morphology of the Li anode, we can believe that the significant enhancement of the cycling stability could be attributed to the artificial protective film, which effectively protects the Li metal from corroding of organic solvent and dissolved O$_2$ during discharge–charge cycles. The obtained promising electrochemical results and scientific understanding show the great promise of developed Li anode protection strategy and would provide design principle and encourage more research for other highly stable Li anodes for practical Li–O$_2$ batteries.

Supporting Information

Supporting Information is available from the Wiley Online Library or from the author.

Acknowledgements

[1] R. S. Assary, J. Lu, P. Du, X. Luo, X. Zhang, Y. Ren, L. A. Curtiss, K. Amine, *ChemSusChem* **2013**, *6*, 51.

[2] J. L. Shui, J. S. Okasinski, P. Keneprotective, H. A. Dobbs, D. Zhao, J. D. Almer, D. J. Liu, *Nat. Commun.* **2013**, *4*, 2255.

[3] R. Younesi, M. Hahlin, K. Edstrom, *ACS Appl. Mater. Interfaces* **2013**, *5*, 1333.

[4] G. Q. Zhang, H. B. Wu, T. Song, U. Paik, X. W. Lou, *Angew. Chem. Int. Ed.* **2014**, *53*, 12590.

[5] J. Liang, X. Y. Yu, H. Zhou, H. B. Wu, S. J. Ding, X. W. Lou, *Angew. Chem. Int. Ed.* **2014**, *53*, 12803.

[6] J. Liu, M. N. Banis, Q. Sun, A. Lushington, R. Li, T. K. Sham, X. Sun, *Adv. Mater.* **2014**, *26*, 6358.

[7] L. Zhao, X. Yu, J. Yu, Y. Zhou, S. N. Ehrlich, Y.-S. Hu, D. Su, H. Li, X.-Q. Yang, L. Chen, *Adv. Funct. Mater.* **2014**, *24*, 5557.

[8] L. Shen, E. Uchaker, X. Zhang, G. Cao, *Adv. Mater.* **2012**, *24*, 6502.

[9] W. Ai, Z. M. Luo, J. Jiang, J. H. Zhu, Z. Z. Du, Z. X. Fan, L. H. Xie, H. Zhang, W. Huang, T. Yu, *Adv. Mater.* **2014**, *26*, 6186.

[10] K. M. Abraham, Z. Jiang, *J. Electrochem. Soc.* **1996**, *143*, 1.

[11] B. Sun, X. Huang, S. Chen, P. Munroe, G. Wang, *Nano Lett.* **2014**, *14*, 3145.

[12] R. Padbury, X. Zhang, *J. Power Sources* **2011**, *196*, 4436.

[13] H.-G. Jung, J. Hassoun, J.-B. Park, Y.-K. Sun, B. Scrosati, *Nat. Chem.* **2012**, *4*, 579.

[14] J. Christensen, P. Albertus, R. S. Sanchez-Carrera, T. Lohmann, B. Kozinsky, R. Liedtke, J. Ahmed, A. Kojic, *J. Electrochem. Soc.* **2012**, *159*, R1.

[15] Y. Shao, F. Ding, J. Xiao, J. Zhang, W. Xu, S. Park, J.-G. Zhang, Y. Wang, J. Liu, *Adv. Funct. Mater.* **2013**, *23*, 987.

[16] J.-S. Lee, S. Tai Kim, R. Cao, N.-S. Choi, M. Liu, K. T. Lee, J. Cho, *Adv. Energy Mater.* **2011**, *1*, 34.

[17] G. Girishkumar, B. McCloskey, A. C. Luntz, S. Swanson, W. Wilcke, *J. Phys. Chem. Lett.* **2010**, *1*, 2193.

[18] a) N. Zhao, C. Li, X. Guo, *Energy Technol.* **2014**, *2*, 317; b) F. Li, T. Zhang, H. Zhou, *Energy Environ. Sci.* **2013**, *6*, 1125.

[19] a) M. Leskes, N. E. Drewett, L. J. Hardwick, P. G. Bruce, G. R. Goward, C. P. Grey, *Angew. Chem. Int. Ed.* **2012**, *51*, 8560; b) S. A. Freunberger, Y. Chen, Z. Peng, J. M. Griffin, L. J. Hardwick, F. Barde, P. Novak, P. G. Bruce, *J. Am. Chem. Soc.* **2011**, *133*, 8040; c) D. Xu, Z. L. Wang, J. J. Xu, L. L. Zhang, L. M. Wang, X. B. Zhang, *Chem. Commun.* **2012**, *48*, 11674.

[20] a) Z.-L. Wang, D. Xu, J.-J. Xu, L.-L. Zhang, X.-B. Zhang, *Adv. Funct. Mater.* **2012**, *22*, 3699; b) Q.-c. Liu, J.-j. Xu, Z.-w. Chang, X.-b. Zhang, *J. Mater. Chem. A* **2014**, *2*, 6081; c) J. J. Xu, Z. L. Wang, D. Xu, L. L. Zhang, X. B. Zhang, *Nat. Commun.* **2013**, *4*, 2438; d) B. Sun, P. Munroe, G. Wang, *Sci. Rep.* **2013**, *3*, 2247; e) D. Su, S. Dou, G. Wang, *NPG Asia Mater.* **2015**, *7*, e155.

[21] a) R. S. Assary, J. Lu, P. Du, X. Luo, X. Zhang, Y. Ren, L. A. Curtiss, K. Amine, *ChemSusChem.* **2013**, *6*, 51; b) J. L. Shui, J. S. Okasinski, P. Keneprotective, H. A. Dobbs, D. Zhao, J. D. Almer, D. J. Liu, *Nat. Commun.* **2013**, *4*, 2255; c) R. Younesi, M. Hahlin, K. Edstrom, *ACS Appl. Mater. Interfaces* **2013**, *5*, 1333.

[22] P. Du, J. Lu, K. C. Lau, X. Luo, J. Bareno, X. Zhang, Y. Ren, Z. Zhang, L. A. Curtiss, Y. K. Sun, K. Amine, *Phys. Chem. Chem. Phys.* **2013**, *15*, 5572.

[23] G. A. Elia, J.-B. Park, B. Scrosati, Y.-K. Sun, J. Hassoun, *Electrochem. Commun.* **2013**, *34*, 250.

[24] W. Walker, V. Giordani, J. Uddin, V. S. Bryantsev, G. V. Chase, D. Addison, *J. Am. Chem. Soc.* **2013**, *135*, 2076.

[25] D. J. Lee, H. Lee, J. Song, M.-H. Ryou, Y. M. Lee, H.-T. Kim, J.-K. Park, *Electrochem. Commun.* **2014**, *40*, 45.

[26] S. J. Kang, T. Mori, J. Suk, D. W. Kim, Y. Kang, W. Wilcke, H.-C. Kim, *J. Mater. Chem. A* **2014**, *2*, 9970.

[27] Z. Peng, S. A. Freunberger, Y. Chen, P. G. Bruce, *Science* **2012**, *337*, 563.

[28] J. Hassoun, H. G. Jung, D. J. Lee, J. B. Park, K. Amine, Y. K. Sun, B. Scrosati, *Nano Lett.* **2012**, *12*, 5775.

[29] H. Nakai, T. Kubota, A. Kita, A. Kawashima, *J. Electrochem. Soc.* **2011**, *158*, A798.

[30] B. D. Adams, C. Radtke, R. Black, M. L. Trudeau, K. Zaghib, L. F. Nazar, *Energy Environ. Sci.* **2013**, *6*, 1772.

[31] Y.-C. Lu, D. G. Kwabi, K. P. C. Yao, J. R. Harding, J. Zhou, L. Zuin, Y. Shao-Horn, *Energy Environ. Sci.* **2011**, *4*, 2999.

[32] B. M. Gallant, D. G. Kwabi, R. R. Mitchell, J. Zhou, C. V. Thompson, Y. Shao-Horn, *Energy Environ. Sci.* **2013**, *6*, 2518.

[33] R. R. Mitchell, B. M. Gallant, Y. Shao-Horn, C. V. Thompson, *J. Phys. Chem. Lett.* **2013**, *4*, 1060.

[34] E. Yilmaz, C. Yogi, K. Yamanaka, T. Ohta, H. R. Byon, *Nano Lett.* **2013**, *13*, 4679.

[35] R. Black, J. H. Lee, B. Adams, C. A. Mims, L. F. Nazar, *Angew. Chem. Int. Ed.* **2013**, *52*, 392.

[36] R. Black, S. H. Oh, J. H. Lee, T. Yim, B. Adams, L. F. Nazar, *J. Am. Chem. Soc.* **2012**, *134*, 2902.

[37] W. Fan, Z. Cui, X. Guo, *J. Phys. Chem. C* **2013**, *117*, 2623.

[38] H. G. Jung, H. S. Kim, J. B. Park, I. H. Oh, J. Hassoun, C. S. Yoon, B. Scrosati, Y. K. Sun, *Nano Lett.* **2012**, *12*, 4333.